

# 3D Building Reconstruction from LiDAR Data

Lu Wang

LiDAR Software Development  
John Chance Land Surveys  
Lafayette, LA 70506

Chee-hung Henry Chu

Center for Advanced Computer Studies  
University of Louisiana at Lafayette  
Lafayette, LA 70504-4330  
Email: cice@cacs.louisiana.edu

**Abstract**—Airborne LiDAR data can be used to create 3D terrain models useful in augmented or virtual reality in which real-world landscapes are incorporated. Automatic generation of 3D models of man-made structures such as buildings is essential for creating these detailed models. We present a method that builds a 3D mesh, segments the triangles, and forms planar facets that correspond to a roof structure of a target building. We illustrate our method with real-world data sets.

**Keywords**—3D reconstruction, segmentation, pattern recognition.

## I. INTRODUCTION

In last few years, the need for 3D visualization in geographical information has received increased attention, especially for viewing urban areas. Such information is being heavily used in a wide range of applications such as urban planning, urban construction, urban change monitoring, and environmental monitoring and protection. Technologies such as immersive visualization, augmented and virtual reality often require that 3D models of urban landscape be modeled and constructed. Creation of such models is labor intensive. Light detection and ranging (LiDAR) surveying systems provide accurate and dense scanning laser points, which can define a good man-made structure profile. A LiDAR scanner traces a narrow laser beam across a regular grid of sample points and measures the arrival time of reflected light for each sample point. Based on this time and the constant speed of light, the scanner can report the 3D position of surface points from a pyramidal region of space [4].

Detailed 3D city model can be made from this aerial LiDAR data. The point cloud acquired by a LiDAR scanner is a set of unstructured points that must be processed into mesh or planar surfaces so that the terrain model can be rendered efficiently. Multiple data sources are typically utilized in order to construct accurate digital representations of urban landscapes. The most common additional source of information is aerial or satellite imagery [19].

An important first step in handling LiDAR data is to segment the data set [7] and to identify the segmented components. Haala and Brenner [5] combine multispectral imagery and laser altimeter data to extract buildings, trees, and grass-covered areas. In an urban landscape, man-made structures such as buildings are often of much interest to a user. As a result, much research efforts have been directed towards extracting such properties as the height and shape of a building from a LiDAR point cloud [10].

Most prior work in this area focused on extracting the shape, or the footprint, of the building. Zhang et al. [6] separate the ground and non-ground LiDAR data points using a progressive morphological filter. Building measurements are identified from non-ground measurements by a region-growing algorithm and plane-fitting technique. Finally, the footprints of buildings are formed by connecting the boundary points. Wang et al. [14] use a Bayesian technique to automatically construct building footprints from a pre-classified LiDAR point cloud. Cheng et al. [17] directly extract the building boundaries from high-resolution imagery and improves the correctness and completeness of the extracted boundaries by integrating LiDAR data.

A building with a flat roof is completely specified by the height and its footprint. In the more general case when the building's roof consists of a number of steeped surfaces, the processing needed is often more sophisticated. Hu et al. [11] describe a hierarchical technique that creates a tree-structured building model composed of geometric primitives extracted from LiDAR data and use aerial imagery to aid the model and refine processes. Jaw and Cheng [18] present a method of building roof reconstruction by fusing laser range data and aerial images through a sequence of Construct-Shape-Refine (CSR) procedures. Vosselman [8] uses a three-dimensional version of the well-known Hough transform to extract planar faces from the irregularly distributed point clouds, and the known ground plans of the buildings are available to support the 3D reconstruction usage. Haithcoat [9] generates the digital surface model (DSM) from the LiDAR point data. Then an orthogonal algorithm is used to extract building footprints and a watershed analysis is conducted to extract the ridge lines of building roofs.

In this paper, we propose a method using airborne LiDAR data as the only data source to reconstruct man-made structure 3d model. Our proposed 3D building reconstruction pipeline assumes that the LiDAR data set has been segmented using methods such as those reported in [3,7] so that a building segment can be identified based on features such as the shape of the footprint. A triangular mesh covering the building is constructed from the laser points. A 2D building outline is extracted from this mesh. Simultaneously, the triangles are pre-processed and clustered to reconstruct planar facets. The planar facets are combined with the 2D building outline to form a 3D building model. The 3D building model is, in turn, combined with a linescan color attribute set to form a textured (or colored) 3D building model.

Further details of the steps in our pipeline are presented in Section 2. We describe experiments and results in Section 3. Finally, we draw our conclusion in Section 4.

## II. 3D BUILDING RECONSTRUCTION

A mesh of triangles is used to represent the LiDAR data. Each laser point in the LiDAR data set is a potential vertex in the mesh. A LiDAR sensor scans the scene and for each scan, it acquires a number of sample points, referred to as beams. Each scan more or less follows a straight line and successive beams on a scan are approximately equally spaced. Thus, each 3D laser point  $(x,y,z)$  is associated with a scan number and a beam number. To build a mesh, for every set of four laser points from adjacent scans and beams, we can create zero, one, or two triangles. We apply a threshold to the elevation differences of the laser points to determine whether one or more triangles are formed. The shorter of the two diagonals is also used to determine how the triangles are generated. Let  $d$  be the diagonal length threshold, if the length of the shorter diagonal is larger than  $d$ , then no triangles would be created. Otherwise, two triplets of points may become triangles. Each triplet of points is made into a triangle only if all the pairwise elevation differences are less than the pre-defined elevation difference threshold (Figure 1).

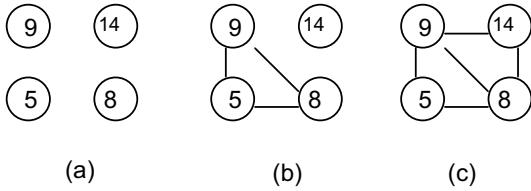


**Figure 1.** An example with four points with the associated elevations. By adjusting the elevation difference threshold, three different scenarios can arise. (a) No triangles are created by setting the threshold to 2. (b) One triangle is created by setting the threshold to 5. (c) Two triangles are created when the threshold is set to 6; in this case, the shorter diagonal is taken.

After the mesh is built, all the external vertices are obtained. Connecting these external vertices in sequence generates the initial building outline. Then, the external vertices are segmented into clusters by computing the slopes of their connected vertices. The best fitting lines from each vertex cluster are generated such that

$$d = \sum_i \|f(x_i; a, b) - y_i\|^2$$

is minimized. By intersecting these best fitting lines, the final building is created. The minimization problem is solved by taking the partial derivatives of  $d$  with respect to  $a$ , and  $b$ , and setting them equal to zero.

### A. Building data segmentation

In order to create the 3D building model, an important step is to create the planar facets of the building roof. To create the planar facets, we need to know which laser points are on the same planar facet. A graph-theoretic segmentation algorithm [1,2] is applied to segment the laser points into different clusters.

Each cluster contains the information of one planar facet. For each triangle in the mesh, we compute its centroid  $V_c$  and unit normal vector  $\mathbf{n}$ . Consider the centroid of each triangle as a node in a graph  $G(V_c, E)$ . The weight associated with each edge  $E$  between a pair node  $w_{ij}$ , is defined as the similarity between node  $i$  and  $j$ . Given two nodes in the graph, we use the dot product of the two normal vectors  $\mathbf{n}_i$  and  $\mathbf{n}_j$  to decide the similarity of these two nodes. The weight between two nodes is computed as:

$$w_{ij} = \begin{cases} e^{-\gamma(1-\mathbf{n}_i \cdot \mathbf{n}_j)^2 / \sigma^2} & \text{if } |V_{c_i} - V_{c_j}| < d \\ 0 & \text{otherwise} \end{cases}$$

where  $\gamma$  is a scale factor,  $\mathbf{n}_i$  is the unit normal vector of triangle  $i$ , the parameter  $V_{c_i}$  is the centroid of triangle  $i$ , and  $d$  is the pre-defined distance threshold.

The centroids of triangles are segmented using normalized cut algorithm [2]. Each partition of laser points represents a planar facet definition of the roof. In graph theoretic framework, the goal of the partitioning is to maximize the similarity within each of the disjoint sets while minimizing the similarity between the two sets. A partition can be evaluated by the cut measure:

$$cut(A, B) = \sum_{\substack{\text{node } i \in A, \\ \text{node } j \in B}} w_{ij}$$

Segmentation by minimizing the cut measure can result in small partitions since a large number of edge cuts resulting from a large partition increases the cut measure. An alternative to the cut measure is the normalized cut measure, defined as:

$$Ncut(A, B) = \frac{cut(A, B)}{assoc(A, V)} + \frac{cut(A, B)}{assoc(B, V)}$$

where

$$assoc(A, V) = \sum_{\substack{\text{node } i \in A, \\ \text{node } j \in V}} w_{ij}$$

Since normalized cut measure discourages the small partitions containing only a few nodes, the segmentation of roof points is less affected by noisy points (e.g. laser points returned from air conditioners) or small facets.

The weight matrix is built from the above weight measure, and we use the eigenvector with the second smallest eigenvalue to bipartition the graph. A current partition can be subdivided and the segmented parts can be recursively repartitioned as needed. The eigenvector corresponding to the next higher eigenvalue is the optimal refinement of the current partition.

### B. 3D model construction

After all the centroids of triangles are partitioned into disjoint clusters, for each cluster of points, we can fit these points to obtain the plane definition. A plane is defined as:

$$ax + by + z = c$$

or

$$z(x_i, y_i; a, b, c) = c - ax - by$$

The problem is now to find the least-squares minimum:

$$E = \sum_i \|z(x_i, y_i; a, b, c) - z_i\|^2$$

The minimized problem is solved by, e.g., taking partial derivatives of  $E$  with respect of  $a$ ,  $b$ , and  $c$ .

The 3D intersection lines between pairs of planes are computed. Combined with 2D building outline, we compute the 2D intersection points of two intersection lines and the 2D intersection points of intersection line and building outline segment. Finally, all the 2D intersection points are projected to each plane to decide the 3D outline of every planar facet of the building.

### C. Linescan color attribute

An integrated line scan camera is typically fitted to a laser scanner. It is used to generate the RGB values for each laser return. A major benefit of this line scan color attribute is that the image geo-referencing process can be bypassed and the color attributes are automatically geo-accurate.

We decompose every planar facet polygon into triangles, and each triangle is recursively decomposed into a set of smaller triangles. All the triangle vertices are matched to the source laser points with linescan color attributes. A triangle is decomposed if 1) its maximum edge length is greater than a pre-defined threshold and 2) its area is greater than a pre-defined threshold. The decomposition rule is to bi-partition the triangle by its shortest median (Figure 2).

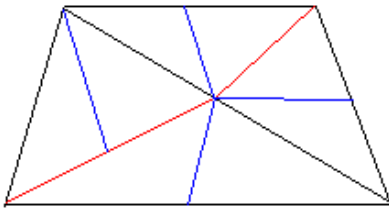


Figure 2. Decompose a facet polygon into a set of triangles

## III. EXPERIMENTAL RESULTS

The system described in the Section II was implemented in software and tested with different LiDAR urban data sets. In the first experiment, the data set shown in Figure 3 contains about 3000 laser points. A triangular mesh (Figure 4) was built from the data set with elevation threshold set at 0.3m.

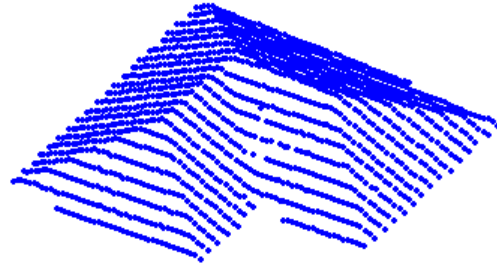


Figure 3. Original LiDAR point cloud.

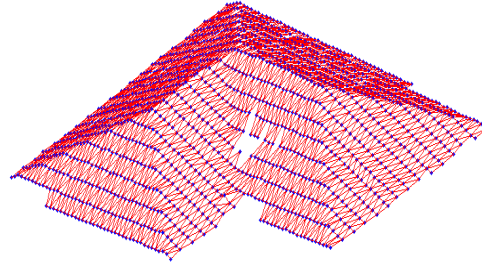


Figure 4. The triangular mesh of the data points.

The test data set is partitioned into 4 segments by applying normalized cut measure twice, as shown in Figure 5. The final segmentation result by the normalized cut measure is shown in Figure 6. The parameters in the normalized cut segmentation were set as:  $\gamma=15.0$ ,  $d=3.0$ ,  $\sigma=2.0$ .

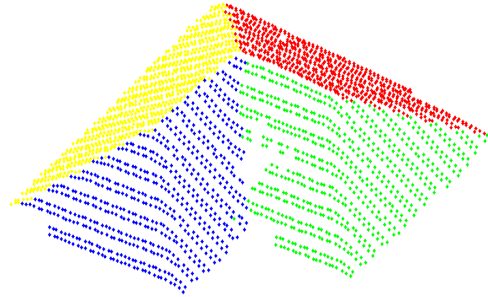
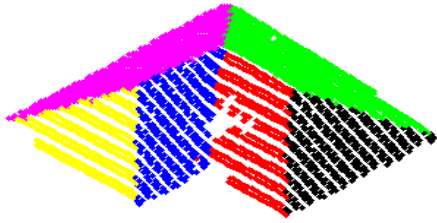
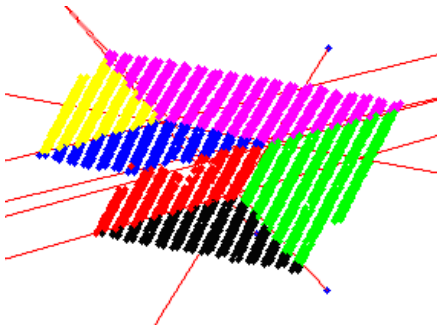


Figure 5. The LiDAR mesh segmented by applying the normalized cut algorithm twice. Each segment is labeled with a unique color for illustration.



**Figure 6.** Building segmentation result.

After the segmentation step, six planar facets were generated, and the intersection lines between planes were computed, which are shown in figures 7 and 8. The final 3D reconstructed building roof model is shown in Figure 9.



**Figure 7.** Intersection lines determined from best fitting planes.

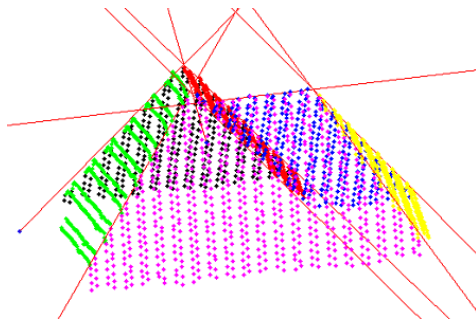


**Figure 8.** Best fitting planes and the intersection lines viewed in 3D.

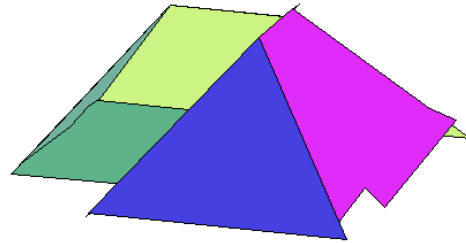


**Figure 9.** 3D reconstructed building model. Each planar surface is labeled with a unique color for illustration.

We also demonstrate another building roof data set containing about 6000 LiDAR laser points (Figure 10). The segmentation results are shown in Figure 11 and the 3D model reconstruction result in Figure 12.

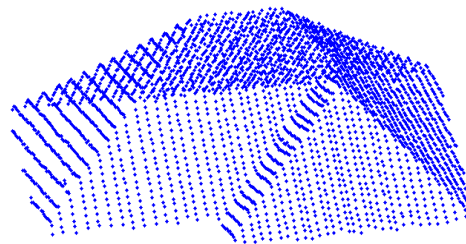


**Figure 10.** A LiDAR set of 6000 points.

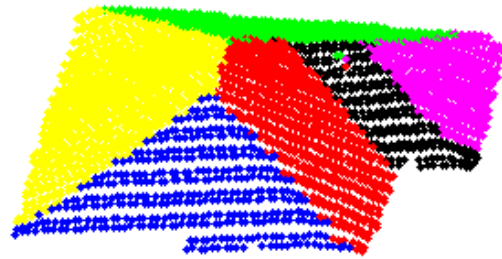


**Figure 11.** Segmentation results of the 6000-point LiDAR set. Each segment is colored with a distinct color.

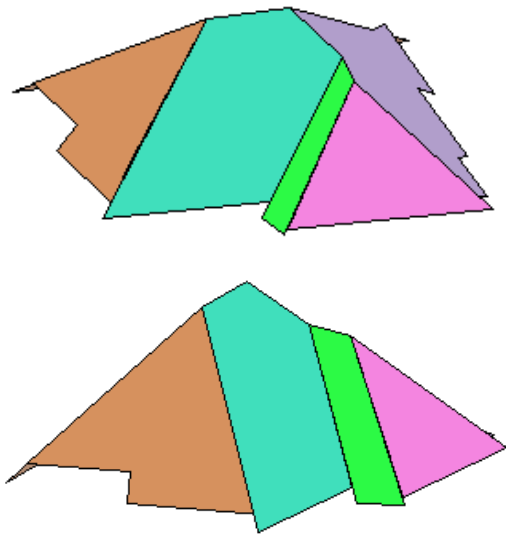


**Figure 12.** Two views of the reconstructed roof from the 6000-point LiDAR set. Each planar surface is colored with a distinct color.

The linescan color attributes of the source laser points are shown in Figure 13. In Figure 14, the vertices of the triangular mesh are colored with the linescan color attributes, which are subsequently applied as texture map to the building's roof (Figure 15). The maximum triangle area is set to  $0.15\text{m}^2$ , and the maximum triangle edge length is set to 1.0m.



**Figure 13.** Source laser points with linescan color attributes.

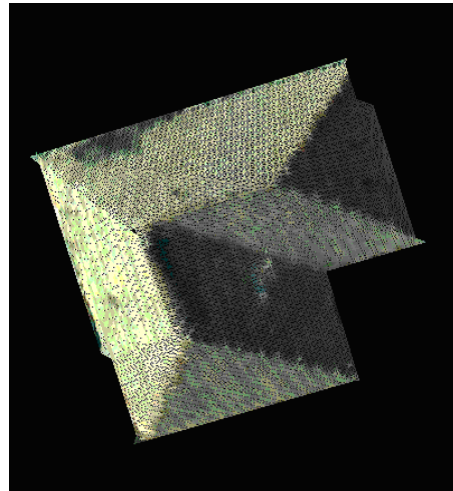


**Figure 14.** All vertices of the decomposed triangles colored with linescan color attributes.

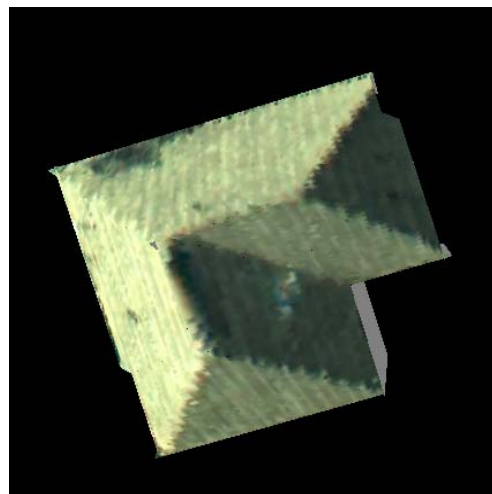


**Figure 15.** Linescan color attributes applied as interpolated color among all vertices using DirectX. This program was developed using DirectX 9.0

#### IV. CONCLUDING REMARKS

We present a method to reconstruct the 3D urban models from LiDAR data. The advantages of this systems are, firstly, only LiDAR data is used in the system, which prevents accumulative errors from other sources; secondly, the segmentation results for the triangles are very stable, since the normal vectors on the same facet are very close to each other, and the segmentation results are affected little by small facets, like the chimneys on the roof or air conditioners, since the normalized cut measure avoids the isolated small partitions; thirdly, the reconstructed 3D building model is by nature a closed structure without extra refinement step or more constraints and requirements, since the outline of each planar

facet is defined from the intersection line with its neighboring planes; last but not least, the processing of the data is fast.

#### ACKNOWLEDGMENT

The authors thank John Chance Land Surveys (JCLS), Inc., for providing the data used in this work. They further thank Kevin Normand, Senior Systems Engineer, supervisor, and Morgan Reed, Senior Systems Engineer, manager at the JCLS LiDAR development department, for their assistance and support.

#### REFERENCES

- [1] Z. Wu and R. Leahy, "An optimal graph theoretic approach to data clustering: Theory and its application to image segmentation," *IEEE Trans. Pattern Analysis and Machine Intelligence*, vol. 15, pp. 1101-1113, 1993.
- [2] J. Shi and J. Malik, "Normalized cuts and image segmentation," *IEEE Trans. Pattern Analysis and Machine Intelligence*, vol. 22, pp. 888 – 905, 2000.
- [3] H. Wei and M. Bartels, "Unsupervised segmentation using Gabor wavelets and statistical features in LiDAR data analysis," in *Proc. 18th International Conference on Pattern Recognition*, I:667-670, 2006.
- [4] B. Lohani, "Airborne Altimetric LiDAR: Principle, Data Collection, Processing and Applications," URL: [http://home.iitk.ac.in/~blohani/LiDAR\\_Tutorial/Airborne\\_AltimetricLiDAR\\_Tutorial.htm](http://home.iitk.ac.in/~blohani/LiDAR_Tutorial/Airborne_AltimetricLiDAR_Tutorial.htm), accessed Feb 2008.
- [5] N. Haala and C. Brenner, "Extraction of building and trees in urban environments," *ISPRS Journal of Photogrammetry and Remote Sensing*, vol. 54, 130-137, 1999.
- [6] K. Zhang, J. Yan, and S. Chen, "Automatic construction of building footprints from airborne LIDAR data," *IEEE Trans. Geoscience and Remote Sensing*, vol. 44, pp. 2523-2533, 2006.
- [7] L. Wang and C.H. Chu, "Graph theoretic segmentation of airborne lidar data," in *Proc. SPIE Defense and Security Symposium*, Orlando, Fla., Apr. 2008.
- [8] G. Vosselman, "3D building model reconstruction from point clouds and ground plans", *International Archives of Photogrammetry and Remote Sensing*, vol. 34, pp. 37-43. 2001.
- [9] T.L. Haithecoat, W. Song, J.D. Hipple, "Building footprint extraction and 3-D reconstruction from LIDAR data," in *Proc. IEEE/ISPRS Joint Workshop Remote Sensing and Data Fusion over Urban Areas*, 2001, pp. 74-78.
- [10] F. Rottensteiner, "Automatic generation of high-quality building models from lidar data", *IEEE Computer Graphics and Applications*, vol. 23, pp. 42-50, 2003.
- [11] J. Hu, S. You, U. Neumann, "Building modeling from LiDAR and aerial imagery," *Proceedings of the ASPRS*, May 2004.
- [12] G. Zhou, C. Song, J. Simmers, and P. Cheng, "Urban 3D GIS from LiDAR and digital aerial images" *Computers & Geosciences*, vol. 30, pp. 345-353, May 2004.
- [13] L.-C. Chen, T.-A. Teo, J.-Y. Rau, J.-K. Liu, W.-C. Hsu, "Building reconstruction from LIDAR data and aerial imagery", in *Proc. IEEE International Geoscience and Remote Sensing Symposium*, vol. 4, pp. 2846- 2849.
- [14] O. Wang, S.K. Lodha, D.P. Helmbold, "A Bayesian approach to building footprint extraction from aerial lidar data", in *Proc. Third International Symposium on 3D Data Processing, Visualization, and Transmission*, June 2006, pp 192-199,
- [15] N. Pfeifer, M. Rutzinger, F. Rottensteiner, W. Mucke, M. Hollaus, "Extraction of building footprints from airborne laser scanning: Comparison and validation techniques," in *Proceedings of the Urban Remote Sensing Joint Event*, Paris, April 2007, pp. 1-9.
- [16] Q.Y. Zhou, and U. Neumann "Fast and extensible building modeling from airborne LiDAR data", in *Proc. ACM SIGSPATIAL International Conference on Advances in Geographic Information Systems (ACM GIS)*, 2008.
- [17] L. Cheng, J. Gong, X. Chen, P. Han, "Building boundary extraction from high resolution imagery and lidar data," *International Archives of the Photogrammetry, Remote Sensing and Spatial Information Sciences*, vol. XXXVII, Part B3b, Beijing, 2008, p.693.
- [18] J.J. Jaw and C.C. Cheng , "Building roof reconstruction by fusing laser range data and aerial images," *International Archives of the Photogrammetry, Remote Sensing and Spatial Information Sciences*, vol. XXXVII, Part B3b, Beijing, 2008, p.707.
- [19] E. Sumer and M. Turker, "Building detection from high-resolution satellite imagery using adaptive fuzzy-genetic approach", in *Geobias'08 Proceeding*, 2008.